

## Wall–colloid interaction in nematic solvents: external field effects

This article has been downloaded from IOPscience. Please scroll down to see the full text article.

2009 J. Phys.: Condens. Matter 21 245105

(<http://iopscience.iop.org/0953-8984/21/24/245105>)

View [the table of contents for this issue](#), or go to the [journal homepage](#) for more

Download details:

IP Address: 129.252.86.83

The article was downloaded on 29/05/2010 at 20:10

Please note that [terms and conditions apply](#).

# Wall–colloid interaction in nematic solvents: external field effects

T G Sokolovska<sup>1,2</sup> and G N Patey<sup>1</sup>

<sup>1</sup> Department of Chemistry, University of British Columbia, Vancouver, BC, V6T 1Z1, Canada

<sup>2</sup> Institute for Condensed Matter Physics, 1 Svientsitskii, Lviv 79011, Ukraine

Received 12 December 2008, in final form 29 March 2009

Published 21 May 2009

Online at [stacks.iop.org/JPhysCM/21/245105](http://stacks.iop.org/JPhysCM/21/245105)

## Abstract

We propose a molecular theory of colloid–wall interactions in nematic media that predicts a new effective force acting on colloidal particles in the presence of an external field. In contrast to the so-called ‘image’ interaction that is always repulsive at long distances, the force identified here can be attractive or repulsive, depending on the type of anchoring at the wall and colloidal surfaces. The effective force on a colloidal particle decreases with distance  $s$  from the wall as  $\exp(-s/\xi)$ , where  $\xi$  is a magnetic (electric) coherence length. At weak fields the force is proportional to  $(\Sigma/\xi)^3$  for ‘quadrupolar’ colloids and to  $(\Sigma/\xi)^2$  for ‘dipoles’, where  $\Sigma$  is the colloidal diameter. A brief discussion of recent experiments in the light of our findings is presented.

Nematic colloids are an important class of materials that are of current interest both for the fundamental questions they pose and because of potential applications [1–3]. A good deal of effort has focused on understanding colloidal interactions and ordering in bulk systems [4–10]. The interactions in bulk systems are now reasonably well understood from both phenomenological [4–6] and molecular [8, 9] viewpoints. A discussion and comparison of both approaches is given in [9].

In the presence of surfaces and applied fields nematic colloids display an amazing variety of phenomena that remain to be understood [3, 11–14]. Obtaining an understanding of the effective forces acting on colloidal particles is a key aspect of the problem. In phenomenological approaches, wall–colloid interactions are described in terms of ‘image’ interactions, analogous to those that occur in electrostatics [15]. At long distances, this description leads to a repulsive force between a colloidal ‘multipole’ and its mirror image in the surface plane, closely akin to the repulsive interaction between an electrostatic multipole and an inert (nonpolarizable) wall. In the present paper, we consider wall–colloid interactions at the molecular level, applying the statistical mechanical approach used in our earlier work [8, 9, 16–20]. We identify a different, field-dependent, wall–colloid interaction which can be attractive or repulsive depending on the particular type of anchoring at the wall and colloidal surfaces. At sufficient range this force will dominate image interactions. We briefly discuss recent experiments [12] in the light of our findings.

We consider a spherical colloidal particle C of diameter  $\Sigma$  in the presence of a wall W as shown in figure 1. The

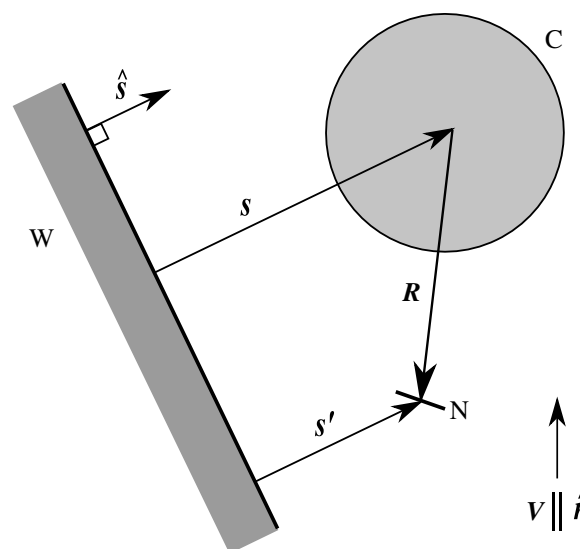


Figure 1. The geometry of the system.

center of the colloidal particle is chosen as the origin of our coordinate system, and an external field  $\mathbf{V}$  defines the  $z$  axis. Sufficiently far from the wall, the bulk director  $\hat{\mathbf{n}}$  (the ‘hat’ denotes a unit vector) is parallel to the field. The vector  $\mathbf{s}$  connects the center of the colloidal particle with the nearest point of the wall surface, and  $\mathbf{s}'$  does the same for a molecule of the nematic N. Note that the wall can take any orientation with respect to the field.

We employ the hypernetted-chain closure familiar in the integral equation theory of liquids [21] in order to obtain the wall–colloid potential of mean force (the effective interaction),  $\phi^{\text{WC}}(s)$ . For the present system the required relationship is

$$-\beta\phi^{\text{WC}}(s) + \beta v^{\text{WC}}(s) = h^{\text{WC}}(s) - c^{\text{WC}}(s) = \int h^{\text{WN}}(s', \hat{\omega}) \rho_{\text{N}}(\hat{\omega}) c^{\text{CN}}(\mathbf{R}, \hat{\omega}) d\mathbf{R} d\hat{\omega}, \quad (1)$$

where  $h^{ij}$  and  $c^{ij}$  are the total and direct correlation functions of components  $i$  and  $j$ ,  $\hat{\omega}$  denotes the orientation of the nematogen,  $\rho_{\text{N}}(\hat{\omega}) = \rho_{\text{N}} f_{\text{N}}(\hat{\omega})$ ,  $\rho_{\text{N}}$  is the nematic number density,  $f_{\text{N}}(\hat{\omega})$  is the orientational distribution of the bulk nematic,  $\beta = 1/k_{\text{B}}T$ , and  $k_{\text{B}}$  is the Boltzmann constant. The term  $\beta v^{\text{WC}}(s)$  represents any direct wall–colloid interaction. This term is not mediated by the nematic and will in general be short-ranged. In the present analysis we are interested in the longer-ranged, nematic-mediated contribution represented by the right-hand side of equation (1), and  $\beta v^{\text{WC}}(s)$  is set to zero. This is not a limitation of the theory, since if for a particular system  $\beta v^{\text{WC}}(s)$  is known and is significant, it can be simply added to our result.

The spirit of our approach [16–20] is to select a molecular model that is analytically tractable, but sufficiently detailed as to trap the basic physics of nematic colloids. The nematogens are modeled as hard particles of diameter  $\sigma$  interacting via an anisotropic soft potential, characterized by energy and length parameters,  $A_{\text{N}}$  and  $z_{\text{N}}$  respectively [16–20]. The nematogens interact with an external field according to

$$v(1) = -V\sqrt{5}P_2(\hat{\omega}_1 \cdot \hat{\mathbf{n}}), \quad (2)$$

where  $P_2$  is the second order Legendre polynomial.

The colloid–nematogen interaction is modeled as

$$v^{\text{CN}}(\mathbf{R}, \hat{\omega}) = \begin{cases} \infty, & R < (\Sigma + \sigma)/2 \\ -A_{\text{C}} \exp[-z_{\text{C}}(R - (\Sigma + \sigma)/2)] P_2(\hat{\omega} \cdot \hat{\mathbf{R}}), & R > (\Sigma + \sigma)/2. \end{cases} \quad (3)$$

where  $\mathbf{R}$  joins the centers of C and N as in figure 1. Note that positive and negative values of  $A_{\text{C}}$  favor perpendicular and parallel orientations of a nematogen with respect to the surface. For  $z_{\text{C}}\sigma = 1$  the colloid–nematogen interaction is of the order of molecular dimensions. The magnitude of  $A_{\text{C}}$  depends on the surfactant concentration on the colloidal surface. Analogously, the wall–nematogen interaction is

$$v^{\text{WN}}(s', \hat{\omega}) = \begin{cases} \infty, & s' < \sigma/2 \\ -A_{\text{W}} \exp[-z_{\text{W}}(s' - \sigma/2)] P_2(\hat{s}' \cdot \hat{\omega}), & s' > \sigma/2, \end{cases} \quad (4)$$

where  $s' = s' \cdot \hat{s}$ . The vectors are defined in figure 1; note that  $s'$  is negative inside the wall.

In order to extract the behavior of the potential of mean force from equation (1) the total correlation function  $h^{\text{WN}}(s, \hat{\omega})$  is required. This was obtained for arbitrary wall orientations in earlier work [16–18]. Expressed as

an expansion in spherical harmonics,  $h^{\text{WN}}(s, \hat{\omega})$  has the form [16, 17]

$$h^{\text{WN}}(s', \hat{\omega}) = \sum_{l,l'=0,2} h_{ll'm}^{\text{WN}}(s') Y_{lm}(\hat{s}') Y_{l'm}^*(\hat{\omega}). \quad (5)$$

The derivation given in [16–18] holds when all correlation lengths are finite, a condition that is met in the presence of an external field. Note that due to the hard core associated with the wall–nematogen interaction,  $h^{\text{WN}}(s, \hat{\omega}) = -1$  for  $s < \sigma/2$ .

The asymptotic behavior of equation (5) at large distances from the wall is given by [20]

$$h^{\text{WN}}(s', \hat{\omega}) \xrightarrow{s' \rightarrow \infty} \frac{h_{221}^{\text{WN}}(s' = \sigma/2)}{Bz_{\text{W}}} [Y_{21}(\hat{s}') Y_{21}^*(\hat{\omega}) + \text{c.c.}] \times \exp[-(s' - \sigma/2)/\xi], \quad (6)$$

where

$$\xi = \sqrt{\frac{K}{V\rho_{\text{N}}S_23\sqrt{5}}} \quad (7)$$

is the magnetic (electric) correlation length,  $K$  is the elastic constant,  $S_2$  is the bulk order parameter,  $B^2 = \langle |Y_{2m}(\hat{\omega})|^2 \rangle_{\omega} \beta K / (15\rho_{\text{N}}S_2^2)$ , and c.c. denotes the complex conjugate of the preceding term. The notation  $\langle \dots \rangle_{\omega}$  indicates  $\int f_{\text{N}}(\hat{\omega})(\dots) d\hat{\omega}$ . For spherical harmonics normalized such that  $Y_{00}(\hat{s}) = 1$ ,  $S_2 = \langle Y_{20}(\hat{\omega}) \rangle_{\omega} / \sqrt{5}$ . The harmonic responsible for the long-range behavior is  $h_{221}^{\text{WN}}(s')$ , and  $h_{221}^{\text{WN}}(s' = \sigma/2)$  is its value at wall–nematogen contact. An explicit expression for the contact value is given in [16, 18]. The other ingredient necessary to obtain the asymptote of  $\phi^{\text{WC}}(s, \hat{\omega})$  is the nematic–colloid direct correlation function, which in the mean spherical approximation (MSA) can be expressed as the expansion

$$c^{\text{CN}}(\mathbf{R}, \hat{\omega}) = \sum_{l,l'=0,2} c_{ll'm}^{\text{CN}}(R) Y_{lm}(\hat{\mathbf{R}}) Y_{l'm}^*(\hat{\omega}). \quad (8)$$

The uniaxial symmetry of the bulk nematic ensures that  $\langle Y_{lm}(\hat{\omega}) Y_{l'm}^*(\hat{\omega}) \rangle_{\omega} = 0$  unless  $m = m'$ . If we rewrite equation (1) taking account only of the long-range properties of  $h^{\text{WN}}$ , for  $s' \gg \sigma$  we obtain

$$-\beta\phi^{\text{WC}}(s) = \frac{h_{221}^{\text{WN}}(s = \sigma/2)}{Bz_{\text{W}}} \exp[\sigma/(2\xi)] \rho_{\text{N}} \langle |Y_{21}|^2 \rangle_{\omega} \times \int \exp[-(s + \mathbf{R}) \cdot \hat{s}/\xi] [Y_{21}(\hat{s}) Y_{21}^*(\hat{\mathbf{R}}) + \text{c.c.}] \times \theta[s - \sigma/2 + \mathbf{R}\hat{s}] c_{221}^{\text{CN}}(R) d\mathbf{R} - \int c^{\text{CN}}(\mathbf{R}, \hat{\omega}) \theta[-s + \sigma/2 - \mathbf{R} \cdot \hat{s}] \rho_{\text{N}} f_{\text{N}}(\hat{\omega}) d\hat{\omega} d\hat{\mathbf{R}}, \quad (9)$$

where we have used  $Y_{lm}^*(\hat{\omega}) = Y_{l-m}(\hat{\omega})$  and  $Y_{00}(\hat{\omega}) = 1$ . The step functions,  $\theta[x]$ , in equation (9) reflect the hard core conditions. Because in the MSA  $c^{\text{CN}}$  decreases at long distances as  $-\beta v^{\text{CN}}$  (exponentially on the length scale of molecular dimensions in our model) the second integral in equation (9) can be neglected for large  $s$ .

Any periodic function can be expanded in Legendre polynomials, therefore we can write

$$\exp[-(s + \mathbf{R}) \cdot \hat{s}/\xi] \theta[s - \sigma/2 + \mathbf{R} \cdot \hat{s}] = \exp(-s/\xi) \sum_l a_l P_l(\hat{\mathbf{R}} \cdot \hat{s}), \quad (10)$$

where

$$a_l = \frac{2l+1}{2} \int_{-1}^1 \exp(-Rx/\xi) \theta\left(s - \frac{\sigma}{2} + Rx\right) P_l(x) dx.$$

Noting that

$$P_l(\hat{\mathbf{R}} \cdot \hat{\mathbf{s}}) = \frac{1}{2l+1} \sum_{m=-l}^l Y_{lm}(\hat{\mathbf{R}}) Y_{lm}^*(\hat{\mathbf{s}}),$$

one obtains

$$-\beta\phi^{\text{WC}}(\mathbf{s}) = 2 \exp[-(s - \sigma/2)/\xi] \rho_N \langle |Y_{21}|^2 \rangle_\omega Y_{21}(\hat{\mathbf{s}}) Y_{21}^*(\hat{\mathbf{s}}) \times \frac{h_{221}^{\text{WN}}(s = \sigma/2)}{Bz_W} \int_0^\infty \tilde{a}_2 c_{221}^{\text{CN}}(R) R^2 dR, \quad (11)$$

where  $\tilde{a}_l = 4\pi a_l / (2l + 1)$ . Since

$$\tilde{a}_2 = 2\pi \begin{cases} \int_{-1}^1 \exp(-Rx/\xi) P_2(x) dx, & R < s - \sigma/2 \\ \int_{-(s-\sigma/2)/R}^1 \exp(-Rx/\xi) P_2(x) dx, & R > s - \sigma/2, \end{cases} \quad (12)$$

the integral in equation (11) can be rewritten as

$$\int_0^\infty \tilde{a}_2 c_{221}^{\text{CN}}(R) R^2 dR = 2\pi \int_0^\infty R^2 dR c_{221}^{\text{CN}}(R) \times \int_{-1}^1 \exp(-Rx/\xi) P_2(x) dx - 2\pi \int_{s-\sigma/2}^\infty R^2 dR c_{221}^{\text{CN}}(R) \times \int_{-1}^{-(s-\sigma/2)/R} \exp(-Rx/\xi) P_2(x) dx. \quad (13)$$

We are interested in the effective potential when the wall–colloid separation is large compared to molecular dimensions,  $s - (\sigma + \Sigma)/2 \gg \sigma$ . For such distances the last integral in equation (13) is negligibly small because the nematic–colloid direct correlation function is short-ranged, and decreases as the potential (equation (3)). Using the integral representation of the Bessel function

$$j_l(kR) = \frac{1}{2i^l} \int_{-1}^1 \exp(ikRx) P_l(x) dx, \quad (14)$$

the first integral in equation (13) can be expressed in terms of the Hankel transform

$$\tilde{c}_{211}^{\text{CN}}(k) = 4\pi i^l \int_0^\infty dR R^2 j_l(kR) c_{211}^{\text{CN}}(R). \quad (15)$$

Thus, we obtain

$$-\beta\phi^{\text{WC}}(\mathbf{s}) = 2\rho_N \langle |Y_{21}|^2 \rangle_\omega Y_{21}(\hat{\mathbf{s}}) Y_{21}^*(\hat{\mathbf{s}}) \exp[-(s - \sigma/2)/\xi] \times \frac{h_{221}^{\text{WN}}(s = \sigma/2)}{Bz_W} \tilde{c}_{221}^{\text{CN}}(k = i/\xi). \quad (16)$$

Equation (16) is valid for colloidal particles of any size. In earlier work [19, 20] we suggested that for sufficiently large colloidal particles (i.e.  $\Sigma \gg z_C^{-1}, z_N^{-1}, \sigma$ )  $c^{\text{CN}}(\mathbf{R}, \hat{\mathbf{w}})$  can be well approximated by the wall–nematic direct correlation function for which we have an analytic form [18]. For a

spherical colloidal particle with a uniform surface, the nematic distribution around the colloid (i.e. the colloid’s ‘nematic coat’) possesses uniaxial up–down symmetry with respect to the director [19]. This is the so-called ‘quadrupole’ configuration frequently observed in experiments.

Hence, for large colloids we employ the explicit expression for  $c_{221}^{\text{CN}}(\mathbf{R}) \approx c_{221}^{\text{WN}}(s = R - \Sigma/2)$  (see equation (20) of [18]). Then, noting that  $j_2(x) = \frac{x^2}{15}(1 - \frac{x^2}{14} + \frac{x^4}{504} - \dots)$ , for weak fields  $\tilde{c}_{221}^{\text{CN}}(k)$  can be expanded at large  $\Sigma$  and small  $k$  to obtain

$$\tilde{c}_{221}^{\text{CN}}(k = i/\xi) \xrightarrow{\xi \gg \Sigma} 4\pi \frac{h_{221}^{\text{WN}}(s = \sigma/2)}{30z_C} B[\Sigma^4/(8\xi) + \Sigma^3 + O(\Sigma^2)] \xi^{-2}. \quad (17)$$

This yields

$$-\beta\phi^{\text{WC}}(\mathbf{s}) = \frac{\pi}{2} \rho_N \langle |Y_{21}|^2 \rangle_\omega \frac{h_{221}^{\text{WN}}(s = \sigma/2) h_{221}^{\text{CN}}(s = \sigma/2)}{z_W z_C} \times \exp[-(s - \sigma/2)/\xi] \sin^2(2\theta_s) \times \xi^{-2} [\Sigma^4/(8\xi) + \Sigma^3 + O(\Sigma^2)], \quad (18)$$

where  $h_{221}^{\text{CN}}(s = \sigma/2)$  is a contact value analogous to  $h_{221}^{\text{WN}}(s = \sigma/2)$ , but with colloidal parameters  $A_C$  and  $z_C$ . Explicit expressions for the contact values of  $h^{\text{CN}}$  and  $h^{\text{WN}}$  are given in [16, 18]. The important observation for our analysis is simply that they are proportional to  $\beta A_C$  and  $\beta A_W$ , respectively. This means that the force acting in the direction normal to the wall on a colloidal particle with quadrupolar symmetry is attractive when  $A_C$  and  $A_W$  have the same sign. That is, colloidal particles with perpendicular anchoring are attracted to tilted walls with similar surface conditions, but repelled from walls with planar anchoring. This is illustrated pictorially for a particular geometry in figure 2 (panel (a)). The magnitude of the force can be written as

$$F^{\text{WC}}(s) = 3\eta \frac{\langle |Y_{21}|^2 \rangle_\omega k_B T h_{221}^{\text{WN}}(s = \sigma/2) h_{221}^{\text{CN}}(s = \sigma/2)}{\sigma (z_W \sigma)(z_C \sigma)} \times \exp\left(\frac{\sigma}{2\xi}\right) \sin^2(2\theta_s) \left[ \frac{\Sigma^4}{8\xi^4} + \frac{\Sigma^3}{\xi^3} + \frac{O(\Sigma^2)}{\xi^3} \right] \times \exp(-s/\xi), \quad (19)$$

where  $\eta = \pi \rho_N \sigma^3 / 6$ . We note that the force vanishes if the tilted wall is parallel or perpendicular to the field, and that the angle of maximum force is  $45^\circ$ . Analysis indicates that the maximum force acting on a colloidal particle at distance  $s = 15\Sigma$  is induced by a field with magnetic (electric) coherence length  $\xi \approx 5\Sigma$ , whereas at shorter distances ( $s = 5\Sigma$ ) the optimal effect requires stronger fields ( $\xi \approx 1.6\Sigma$ ).

It is important to ask if these forces are strong enough to have significant physical effects that might be observed experimentally. To address this question, we calculate the force for the model parameters  $z_C \sigma = z_W \sigma = z_N \sigma / 2 = 0.5$ ,  $\beta A_N = 1$ ,  $\beta A_C = \beta A_W = 4$ . These correspond to interactions that decay on length scales of the order of nematogen dimensions, nematogen–nematogen interactions of order  $k_B T$ , and surface–nematogen interactions of order  $4k_B T$ . We would expect these values to roughly describe a ‘typical’ system with moderate surface anchoring. For these parameters  $\beta A_N \eta \langle |Y_{21}|^2 \rangle_\omega = 0.312$  [18] and  $h_{221}^{\text{WN}}(s = \sigma/2) = h_{221}^{\text{CN}}(s = \sigma/2) \approx 2$  [16].

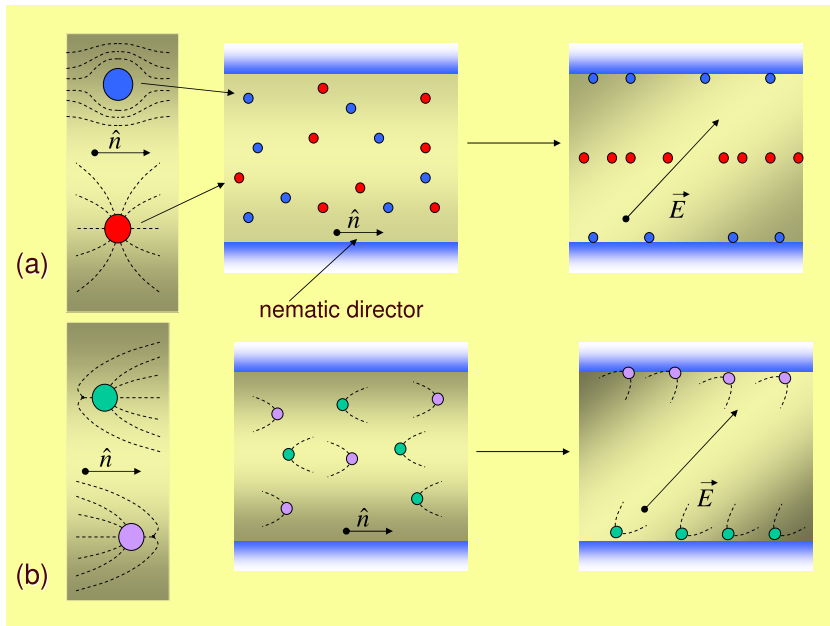


**Figure 2.** A pictorial illustration of the influence of an electric field  $\vec{E}$  on colloidal particles immersed in a slab of nematic fluid.  $\hat{n}$  indicates the direction of the bulk director, and the walls are ‘treated’ to ensure planar anchoring at zero field. Panel (a) illustrates the situation for quadrupolar colloids with planar (blue, light) and perpendicular (red, dark) surface anchoring. The dashed lines indicate the nematic ordering about the colloidal particles. Note that the blue particles are attracted to the surfaces and the red ones are repelled. Panel (b) illustrates the dipolar colloid case with broken up–down symmetry. Both ‘positive’ (green, dark) ( $\hat{A}_C = D > 0$ ) and ‘negative’ (lilac, light) ( $\hat{A}_C = -D$ ) are shown. Note that for the geometry used in this sketch the positive and negative dipoles are attracted to different surfaces.

(This figure is in colour only in the electronic version)

Then at 300 K and distance  $s = 10\Sigma$ , the estimated force is  $\sim 0.1$  pN at the optimal coherence length  $\xi \approx 3.3\Sigma$ . In this calculation we have taken the nematogen ‘size’ to be of the order of 1 nm. For comparison, we have estimated the so-called image force [15] between a spherical colloid and its mirror image reflected in a surface identical to that of the colloid (the colloid–image distance is  $20\Sigma$ ). For this configuration the image force at zero field (estimated using the quadrupole–quadrupole interaction given in [9]) is 3–4 orders of magnitude weaker than the force described above.

Thus, the force we identify here is of sufficient range and magnitude to be of physical significance, and should be observable in experiments. We believe that the origin of this force is the nonuniform nematic distribution created by tilted walls. As noted above, in our model the long-range force vanishes for wall orientations that are parallel and perpendicular to the field, and some discussion of why this might be so is required. Suppose, for example, that the wall supports perpendicular anchoring ( $A_W > 0$ ), then one would not expect a significant force for a perpendicular field, because if the wall and field act in the same direction no long-range distortions are induced in the nematic. The parallel field case is surprising at first sight because for this orientation the wall and field oppose each other, and distortions are induced in the nematic. However, in earlier work [16] we have shown that for this configuration the distortions tend to be localized near the surface and do not extend far into the nematic. In other words, except near the wall the field dominates. This perhaps explains why the asymptotic force we identify above vanishes for this configuration.

For tilted walls the situation is different. As discussed in [17], tilting the wall breaks the symmetry of the system, and long-range distortions are induced in the nematic. At zero field, the tilted wall reorients the bulk director to create a new uniform nematic distribution. Likewise the nematic coat surrounding a colloid simply rotates without distortion and no force is generated. This is why the force given by equation (19) vanishes at zero field ( $\xi = \infty$ ) for all orientations. At nonzero field (finite  $\xi$ ) the wall-induced nematic deformation remains relatively long-ranged, but the distribution is no longer uniform. Distortions of the nematic distribution are stronger nearer the wall, and these in turn induce a nonuniform deformation in the nematic coat of a colloidal particle. We believe that these distortions drive the force that pushes a colloidal particle towards or away from the wall.

Above we have described a system where the colloid-induced distribution of the surrounding nematic possesses up–down symmetry with respect to the director, the ‘quadrupolar’ case. It is interesting to consider the so-called ‘dipolar’ situation where this symmetry is broken. In the context of our model this can be done by simply redefining the parameter  $A_C$  in equation (3) as  $A_C = \hat{A}_C / \cos \theta_R$ , where  $\theta_R$  is the polar angle defining the orientation of  $\mathbf{R}$  with respect to the director, and  $\hat{A}_C$  is a constant. This model is chosen for convenience because it allows the effective wall–dipole interaction to be obtained with a simple transformation of the quadrupole result discussed above. We emphasize that our objective here is to determine how the wall–colloid interaction changes qualitatively when up–down symmetry is broken, and

for this purpose it is not necessary to specify exactly the physical origin of the broken symmetry. Nevertheless, one can imagine physical situations that would roughly correspond to our model, for example a nonuniform distribution of surfactant over the colloidal surface. In our model nematogens will be ordered parallel to the colloidal surface at one pole and perpendicular at the other. Such a distribution will generate a ‘positive’ dipole in the direction of  $\hat{n}$ , with its ‘hedgehog’ directed downward, if  $\bar{A}_C$  is positive and vice versa if  $\bar{A}_C$  is negative.

Noting that  $Y_{21}(\hat{R}) = \sqrt{5}Y_{11}(\hat{R})/\cos\theta_R$ , and that in the MSA  $c^{\text{CN}}$  is proportional to  $\beta A_C$ ,  $c_{221}^{\text{CN}}(R)Y_{21}(\hat{R})Y_{21}^*(\hat{\omega})$  in expansion (8) transforms into  $\sqrt{5}c_{121}^{\text{CN}}(R)Y_{11}(\hat{R})Y_{21}^*(\hat{\omega})$ , where  $c_{121}^{\text{CN}}$  is just  $\bar{c}_{221}^{\text{CN}}(R)$  calculated for  $\bar{A}_C$ . Equation (16) then transforms to give the wall–dipole result

$$-\beta\phi^{\text{WC}}(s) = 2\sqrt{5}\rho_N(|Y_{21}|^2)_\omega Y_{21}(\hat{s})Y_{11}^*(\hat{s}) \times \exp[-(s - \sigma/2)/\xi] \frac{h_{221}^{\text{WN}}(s = \sigma/2)}{Bz_W} \bar{c}_{211}^{\text{CN}}(k = i/\xi), \quad (20)$$

where

$$\bar{c}_{121}^{\text{CN}}(k = i/\xi) = 4\pi i \int_0^\infty dR R^2 j_1(kR) \bar{c}_{221}^{\text{CN}}(R). \quad (21)$$

Again using the explicit expression for our ansatz [18] and taking into account that  $\xi > \Sigma \gg \sigma$ , one finds

$$\bar{c}_{121}^{\text{CN}}(k = i/\xi) \approx -\pi \frac{\bar{h}_{221}^{\text{CN}}(s = \sigma/2)}{z_C} \times B[\Sigma^3/(6\xi) + \Sigma^2 + O(\Sigma)]\xi^{-1}. \quad (22)$$

The notation in equations (20) and (22) is the same as that used above (equation (17)), except that now the contact value  $\bar{h}_{221}^{\text{CN}}(\sigma/2)$  is proportional to  $\beta\bar{A}_C$  instead of to  $\beta A_C$ . Thus, we obtain

$$\beta\phi^{\text{WC}}(s) = 15\pi\rho_N(|Y_{21}|^2)_\omega \frac{h_{221}^{\text{WN}}(s = \sigma/2)\bar{h}_{221}^{\text{CN}}(s = \sigma/2)}{z_W z_C} \times \exp[-(s - \sigma/2)/\xi] \sin^2(\theta_s) \cos(\theta_s) \times \xi^{-1}[\Sigma^3/(6\xi) + \Sigma^2 + O(\Sigma)]. \quad (23)$$

It follows from equation (23) that ‘positive dipoles’ ( $\bar{A}_C > 0$ ) are repelled from walls with perpendicular anchoring ( $A_W > 0$ ) and attracted to walls with planar anchoring ( $A_W < 0$ ) for positive values of  $\cos\theta_s$ . The physically significant implication of equation (23) is illustrated in figure 2 (panel (b)) for a slab with planar anchoring. The behavior of the colloidal particles illustrated in the figure appears qualitatively consistent with recently reported phenomena [12]. In a cell with planar anchoring, where a series of electrical field envelopes induce director tilt, colloidal particles with wall-facing hedgehogs (‘positive’ dipoles for  $\cos(\theta_s) > 0$ ) were attracted towards the surface.

To summarize, in this paper we have developed a molecular theory of effective, field-dependent, wall–colloid interactions in nematic media. If the preferred nematic orientation imposed by the wall does not coincide with the director dictated by the external field, we have shown that new forces appear and act over significant distances. Unlike so-called ‘image’ interactions [15] these forces can be attractive

as well as repulsive depending on the type of anchoring at the wall and colloidal surfaces. A clear understanding of this effect opens possibilities for manipulating colloidal particles in nematics. The symmetry of the colloid-induced nematic distribution (the colloidal coat) determines the diameter dependence of the wall–colloid interaction, and influences the dependence on the angle  $\theta_s$ , which describes the orientation of the wall normal with respect to the director. In the present analysis the orientation of the bulk director is defined by an external field. The effective force decreases with the distance  $s$  from the wall as  $e^{-s/\xi}$ , where  $\xi$  is a magnetic (electric) coherence length. For weak fields, the force is proportional to  $(\Sigma/\xi)^3$  for ‘quadrupolar’ colloids and to  $(\Sigma/\xi)^2$  for ‘dipoles’. We believe that nonuniformities in the nematic distribution caused by mismatching wall and field influences drive the wall–colloid forces identified here.

## Acknowledgments

Acknowledgment is made to the Donors of the American Chemical Society Petroleum Research Fund for partial support of this research. The financial support of the Natural Science and Engineering Research Council of Canada is gratefully acknowledged.

## References

- [1] Poulin P, Stark H, Lubensky T C and Weitz D A 1997 *Science* **275** 1770
- [2] Stark H 2001 *Phys. Rep.* **351** 387
- [3] Musevic I, Skarabot M, Tkalec U, Ravnik M and Zumer S 2006 *Science* **313** 954
- [4] Ramaswamy S, Nityananda R, Raghunathan V A and Prost J 1996 *Mol. Cryst. Liq. Cryst. Sci. Technol. A* **288** 175
- [5] Ruhwandl R W and Terentjev E M 1997 *Phys. Rev. E* **55** 2958
- [6] Lubensky T C, Pettey D, Currier N and Stark H 1998 *Phys. Rev. E* **57** 610
- [7] Smalyukh I I, Lavrentovich O D, Kuzmin A N, Kachynski A V and Prasad P N 2005 *Phys. Rev. Lett.* **95** 157801
- [8] Sokolovska T G, Sokolovskii R O and Patey G N 2006 *Phys. Rev. E* **73** 020701(R)
- [9] Sokolovska T G, Sokolovskii R O and Patey G N 2008 *Phys. Rev. E* **77** 041701
- [10] Zhou C, Yue P and Feng J J 2008 *Langmuir* **24** 3099
- [11] Loudet J C and Poulin P 2001 *Phys. Rev. Lett.* **87** 165503
- [12] Pishnyak O P, Tang S, Kelly J R, Shiyanovskii S V and Lavrentovich O D 2007 *Phys. Rev. Lett.* **99** 127802
- [13] Ognysta U, Nych A, Nazarenko V, Musevic I, Skarabot M, Ravnik M, Zumer S, Poberaj I and Babic D 2008 *Phys. Rev. Lett.* **100** 217803
- [14] Vilfan M, Osterman N, Copic M, Ravnik M, Zumer S, Kotar J, Babic D and Poberaj I 2008 *Phys. Rev. Lett.* **101** 237801
- [15] Terentjev E M 1995 *Phys. Rev. E* **51** 1330
- [16] Sokolovska T G, Sokolovskii R O and Patey G N 2005 *J. Chem. Phys.* **122** 034703
- [17] Sokolovska T G, Sokolovskii R O and Patey G N 2004 *Phys. Rev. Lett.* **92** 185508
- [18] Sokolovska T G, Sokolovskii R O and Patey G N 2006 *J. Chem. Phys.* **125** 034903
- [19] Sokolovska T G, Sokolovskii R O and Patey G N 2005 *J. Chem. Phys.* **122** 0124907
- [20] Sokolovska T G, Sokolovskii R O and Patey G N 2007 *Condens. Matter Phys.* **10** 407
- [21] Hansen J P and McDonald I R 1986 *Theory of Simple Liquids* (London: Academic)